Electronic Supplementary Information

In situ 3D X-ray imaging of water distribution in each layer of a membrane electrode assembly of a polymer electrolyte fuel cell

Hirosuke Matsui,[a,b] Tomoro Ohta,[a,b] Takahiro Nakamura,[a] Tomoya Uruga,[c] and Mizuki Tada*[a,b]*

[a.] Department of Chemistry, Graduate School of Science & Research Center for Materials Science (RCMS) & Integrated Research Consortium on Chemical Science (IRCCS) & Reaction Infography (R-ing) World Research Unit, Nagoya University, Furo, Chikusa, Nagoya, Aichi 464-8602 (Japan).

[b.] RIKEN SPring-8 Center, SPring-8, Koto, Sayo, Hyogo 679-5198 (Japan).

[c.] Japan Synchrotron Radiation Research Center, SPring-8, Koto, Sayo, Hyogo 679-5198 (Japan).

E-mail: matsui.hirosuke.x1@f.mail.nagoya-u.ac.jp, tada.mizuki.u6@f.mail.nagoya-u.ac.jp

Supplementary Methods

PEFC sample

The three-layered membrane electrode assembly (MEA) was commercially prepared by EIWA Co. Catalyst-coated membranes (3 cm × 3 cm) with electrocatalysts (cathode: 50 wt% Pt/C (TEC10E50E, Tanaka Kikinzoku Kogyo K.K. (TKK)), 3.0 mg_{Pt} cm^{-2}; anode: 50 wt% Ru/C (TECRu(ONLY)50E, TKK), 0.5 mg_{Ru} cm^{-2}) were prepared by spray coating on a PTFE sheet and hot pressed with a Nafion membrane (NR-212, Sigma-Aldrich; 7 cm × 7 cm) to form the three-layered MEA. At both sides of the MEA, pieces of carbon paper (TGP-H-030, Toray Ind. Inc.) coated with 10 wt% PTFE were inserted as gas diffusion layers (GDLs). The MEA with the GDLs was installed in a PEFC cell customized for *in situ* X-ray computed tomography (CT) measurements with $\theta = \pm 80°$. The PEFC cell consisted of Al–Mg separators, Kapton thin-film heaters, Au-coated Cu current collectors, and carbon gas flow channel plates (1 mm × 1 mm, serpentine pattern) (Fig. S1(b)).

Electrochemical experiments

The cell voltage and current were monitored and controlled by a potentiostat/galvanostat (VSP-300, BioLogic Science Instruments Co. Ltd.) with two sets of 10 A booster boards. The cell voltage was controlled by a two-electrode system using the anode as a pseudo-reference electrode. The PEFC cell with the MEA was operated at 353 K by supplying humidified H_2 (>99.99999%) at 250 ccm to the anode and humidified N_2 (>99.99995%) or humidified 20% O_2 in N_2 (>99.99995%) at 1000 ccm to the cathode. The gas humidity was calculated as relative humidity by controlling the temperatures of the humidifying chambers. To avoid the aggregation of water vapor before the inlets of the PEFC cell, the gas lines leading to the PEFC cell were heated at 368 K. The MEA in the PEFC cell was conditioned by 150 *I–V* cycles in 11 steps (0−1.1 A cm^{-2}) for 6 s each. After the conditioning process, the electrochemical performance of the MEA was evaluated. The electrochemically active surface area (ECSA) estimated from the average charge of the hydrogen adsorption and desorption cyclic voltammetry (CV) peaks (0.05−1.00 V at 0.05 V s^{-1}) was 56.4 m^2 g_{Pt}^{-1} (Fig. S2). The maximum power density estimated from the *I–V* profile was 0.35 W cm^{-2}.

***In situ* X-ray CT imaging**

In situ X-ray CT measurements of the operating PEFC cell were performed at the BL36XU beamline of SPring-8 (Fig. S1(a)). Hard X-rays monochromatized by a Si(111) channel-cut compact monochromator were irradiated to the *in situ* PEFC cell with an X-ray transmission window (1 mm width) through a paper rotary diffuser. The *in situ* PEFC cell was mounted on automatic stages (*X*′, *Y*′, and *Z*′) and a rotary stage (θ) along the *Z*′ axis. The stage axes were defined as parallel to the membrane surface (*X*′ and *Z*′) and parallel to the direction of the X-ray optical path (the same as the depth direction of the membrane, *Y*′) (Fig. S3). Perpendicular irradiation of the X-rays to the membrane was defined

as $\theta = 0°$. The X-rays transmitted through the *in situ* PEFC cell were monitored by a high-resolution X-ray imaging unit (scintillator: single-crystalline cerium-doped gadolinium aluminum gallium garnet; lens: AA50, Hamamatsu Photonics K.K.) coupled with an optical lens (×10) and a low-noise sCMOS camera (2048 pixels × 2048 pixels, ORCA-Flash4.0 V2, Hamamatsu Photonics K.K.). The effective pixel size was 0.65 μm × 0.65 μm, with a field of view of 1.33 mm × 1.33 mm. The X-ray energy was set to 9.0 keV for the *in situ* CT imaging, considering the X-ray beam flux at the BL36XU station and the cross-sectional density of the X-ray absorption for the water relative to the PEFC sample.

The CT data sets were composed of the 3D matrices ($I(X'Z'\text{-}\theta)$) of the sample projection images ($X'Z'$) during the rotary scanning of the PEFC (θ) over a range of ±80° with a step interval of 0.1° (1600 images). The camera rate (synchronized with the pulse rate of the θ scanning) was set at 50 Hz and the total acquisition time was approximately 32 s (1600 images × 0.02 s shot^{-1}). X-ray intensity images ($I_0(X'Z')$) were similarly measured without the PEFC cell (sample) in the X-ray optical path. The dark signal of the sCMOS camera ($I_{\text{dark}}(X'Z')$) was measured by closing the X-ray optical shutter.

Initially, the CT data were recorded for the dry MEA under low RH (under N_2 flow to the cathode with RH = 64%). Next, similar CT measurements were conducted under wet conditions by supplying humidified gases (RH = 90% or 100%) to the PEFC cathode by controlling the temperature of the humidifier. During the measurements of the CT data series, the inlets and outlet of the PEFC cell were closed using stop valves to avoid fluctuation and further production of water in the PEFC.

Processing of X-ray CT imaging data

The CT data were recorded at 16-bit depth and the data size was 13 GB in total. A custom-made GPU program with a commercial GPU board (GeForce RTX 3080, NVIDIA) was used for the imaging data analysis. The imaging data were subjected to the following four steps. The details of the data structure and processing are summarized in Figs. S3 and S4.

Step 1: Conversion to the X-ray absorption coefficient

The X-ray transmission images of the MEA for the sample projection angle scan ($I(X'Z'\text{-}\theta)$), the X-ray intensity images recorded without the sample ($I_0(X'Z')$), and the dark signal image of the sCMOS camera ($I_{\text{dark}}(X'Z')$) were used to estimate the X-ray absorption coefficient of the sample ($\mu t(X'Z'\text{-}\theta)$) based on the Beer–Lambert law (eq. S1):

$$\mu t(X'Z' - \theta) = -\ln \frac{I(X'Z' - \theta) - I_{dark}(X'Z')}{I_0(X'Z') - I_{dark}(X'Z')} \qquad \text{(eq. S1)}$$

The converted $\mu t(X'Z'\text{-}\theta)$ data obtained during operation of the PEFC at RH = 90% or 100% (wet) and RH = 64% (dry) were defined as μt_{wet} and μt_{dry}, respectively.

Step 2: Reslicing to obtain sinograms for CT reconstruction

To obtain sinogram images for the 3D reconstruction, the $\mu t(X'Z'\text{-}\theta)$ matrix was resliced to the $X'\theta$ cross-section with the Z' axis ($\mu t(X'\theta\text{-}Z')$).

Step 3: 3D reconstruction by the OS-EM method

The converted sinograms were individually reconstructed into real-space coordinates (XYZ) with the plane of the membrane sample (XZ) orthogonal to the depth (Y) by CT calculations using the ordered subset expectation maximization (OS-EM) method. [S1] Considering calculation cost and data quality, the imaging data were divided into 16 subsets and the number of iterative reconstructions for each subset was 20. The 3D reconstructed images recorded under dry and wet conditions were defined as $\mu t_{dry}(XYZ)$ and $\mu t_{wet}(XYZ)$, respectively.

Step 4: Extraction of the images of water distribution in the PEFC

The 3D images of the water distribution in the PEFC ($\mu t_{H2O}(XYZ)$) were calculated as the difference between $\mu t_{dry}(XYZ)$ and $\mu t_{wet}(XYZ)$ (eq. S2):

$$\mu t_{H2O}(XYZ) = \mu t_{wet}(XYZ) - \mu t_{dry}(XYZ) \qquad \text{(eq. S2)}$$

Because we acquired the CT data sets under dry and wet conditions in the same field of view, we could subtract the common sample structure image, and the residual intensity after subtraction (eq. S2) was regarded as originating from the X-ray absorption of water in the PEFC. To detect the absorption of water, we used a custom-made analytical program (OpenCV with CUDA library) with the six-dimensional affine transformation of the 3D imaging data to correct the field of view between the raw data (translation: $T_X T_Y T_Z$) and sample swelling due to water (magnification scaling: $S_X S_Y S_Z$). The X-ray signal level outside the MEA and GDLs was set as the threshold, and the intensity greater than the threshold was regarded as water inside the sample. The X-ray absorption of the MEA sample was approximately 15 times larger than that detected as water.

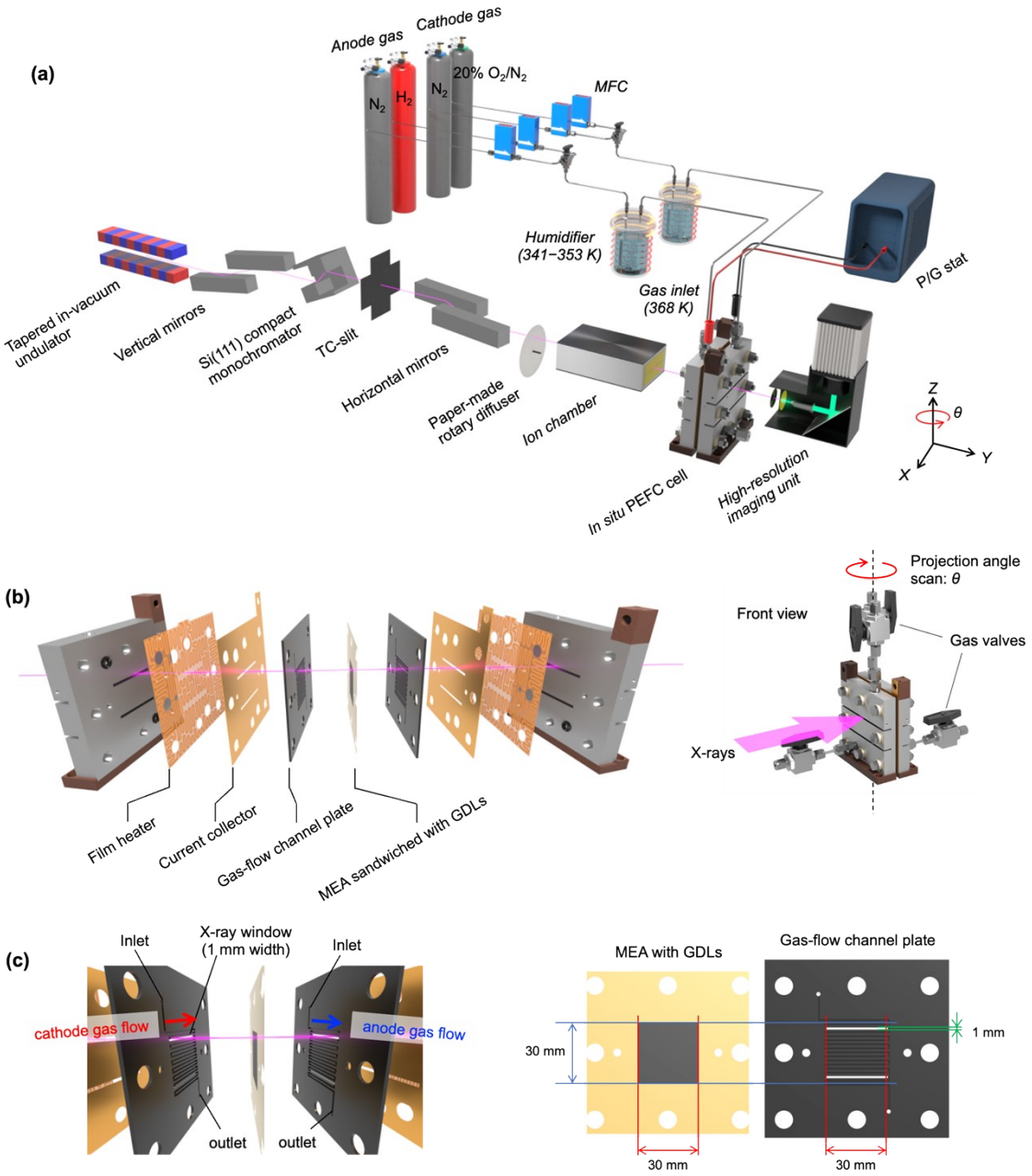

Fig. S1 (a) Schematic illustration of the experimental setup for the *in situ* X-ray CT measurements at the SPring-8 BL36XU beamline. (b) Structure of the *in situ* PEFC cell for the X-ray CT measurements. (c) Schematic illustration of the gas channels at the cathode and anode sides of the PEFC cell relative to the X-ray irradiation direction.

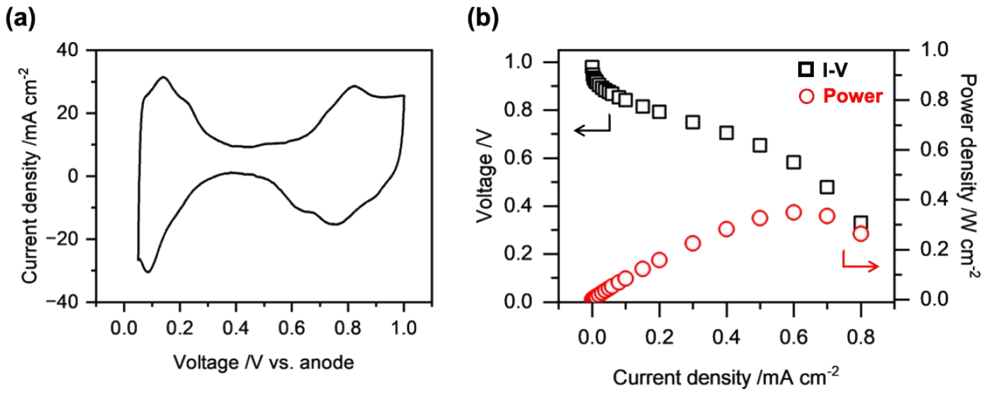

Fig. S2 (a) CV and (b) I–V profiles of the MEA used for the *in situ* X-ray CT measurements.

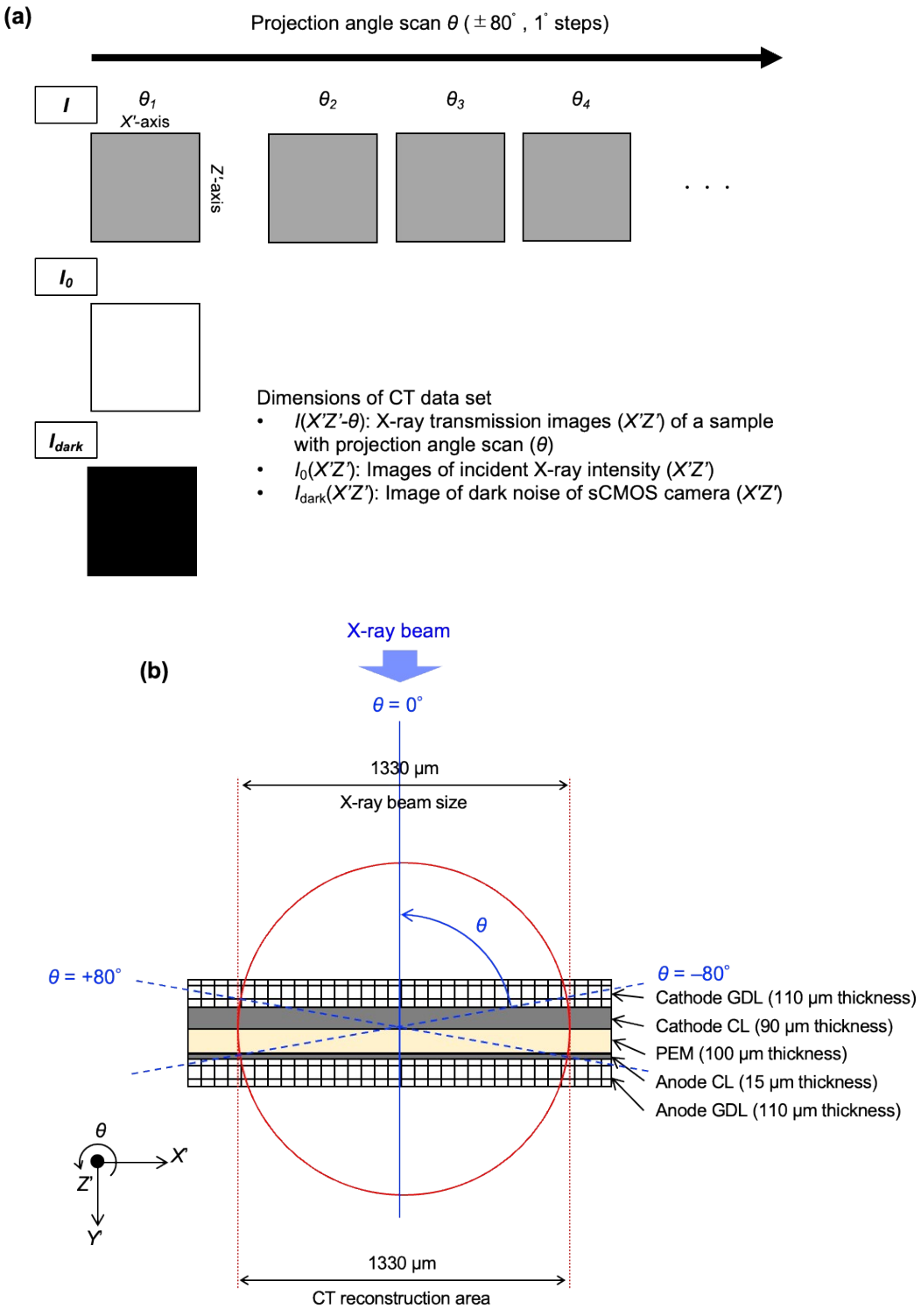

Fig. S3 (a) Details of a CT data set. (b) Schematic diagram defining the X-ray CT measurement axes.

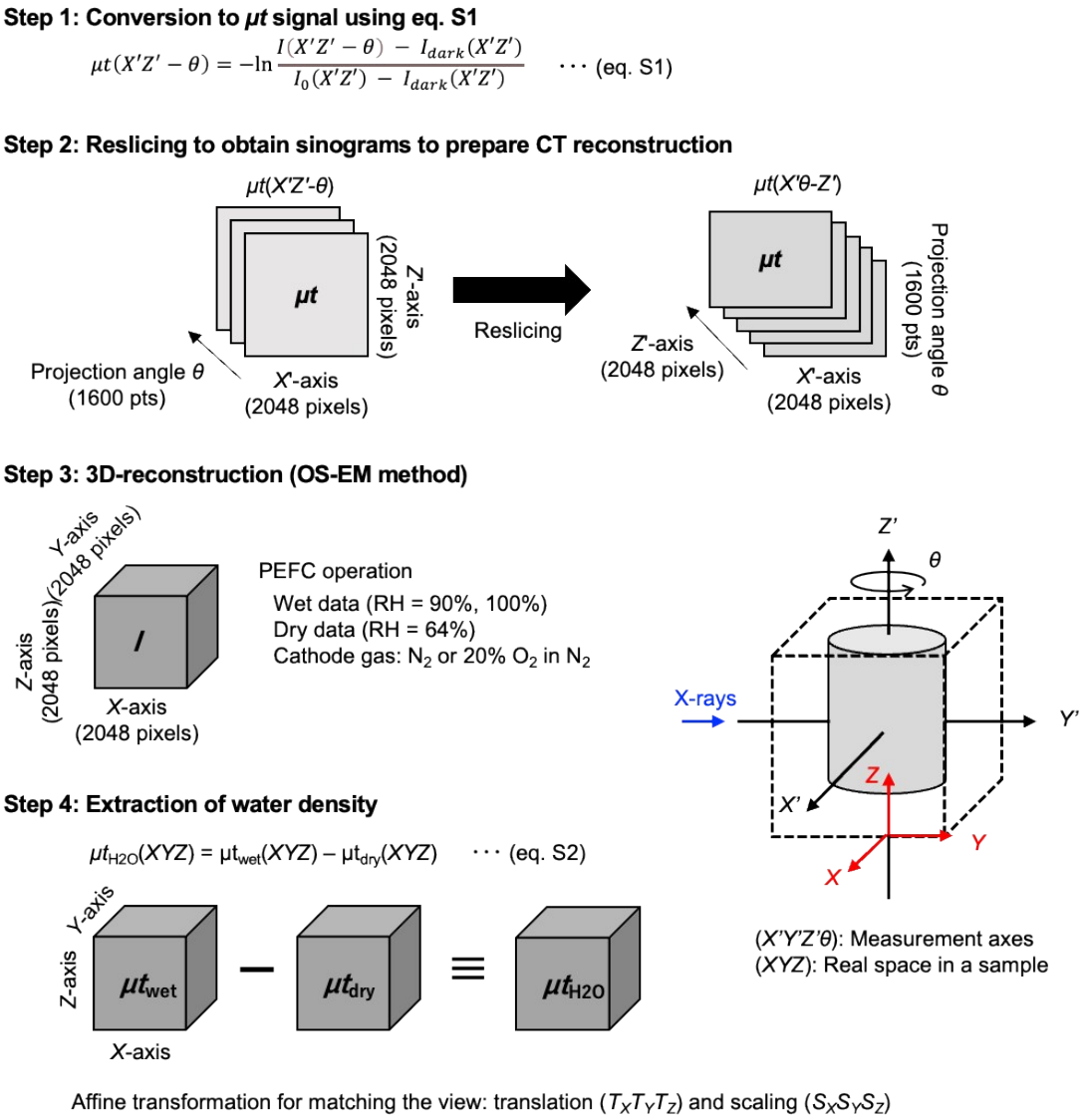

Fig. S4 Analytical procedure for the X-ray CT imaging of water in the PEFC (OS-EM: ordered subset expectation maximization).[S1]

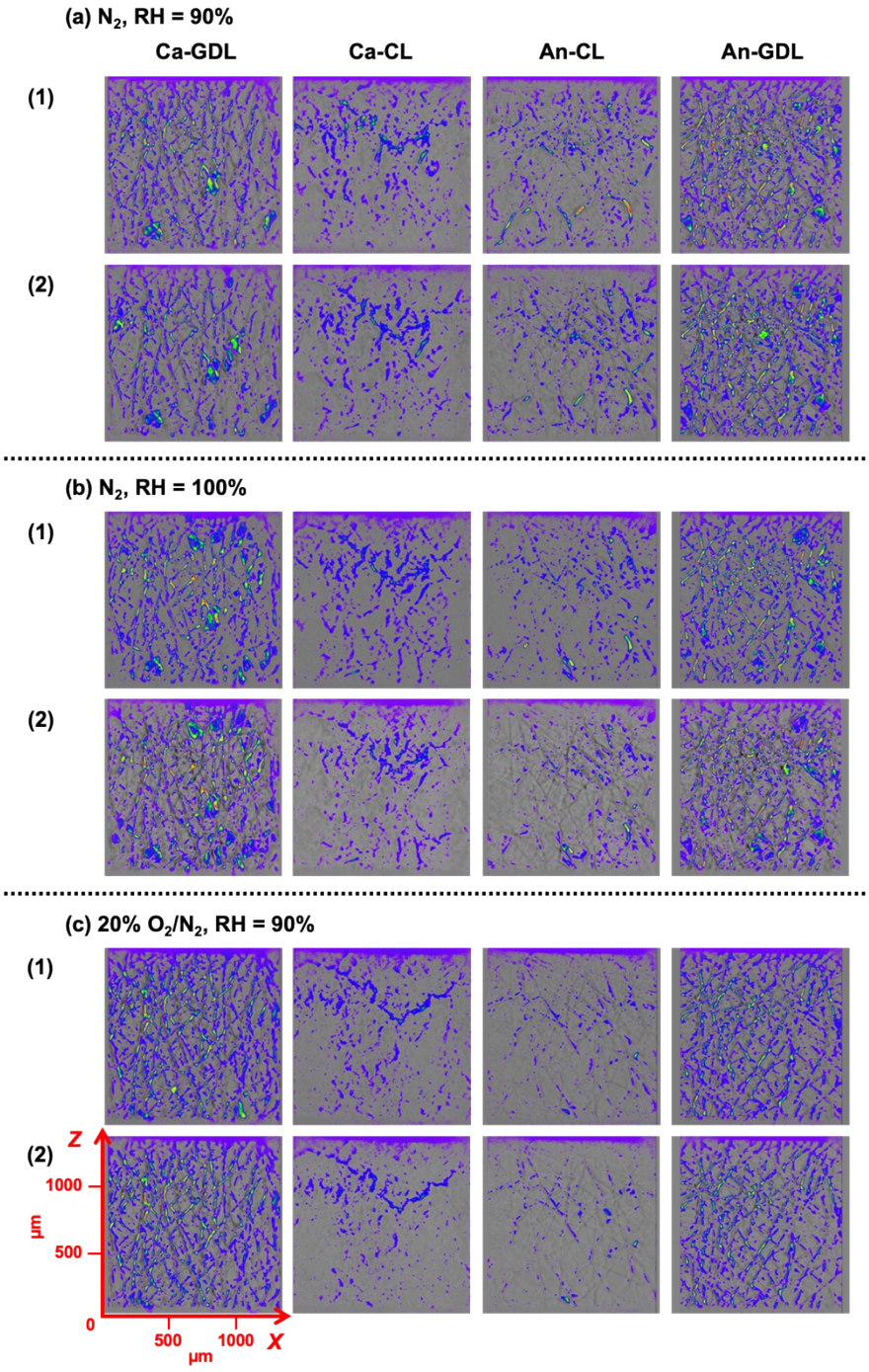

Fig. S5 Other examples (1, 2) of 2D cross-sectional images of the water distribution at various depths (Y), corresponding to the cathode gas diffusion layer (Ca-GDL, Y = 50 μm), cathode catalyst layer (Ca-CL, Y = 155 μm), anode CL (An-CL, Y = 308 μm), and anode GDL (An-GDL, Y = 380 μm). Y = 0 μm was defined as the depth of the surface of the cathode GDL. The CT data sets of the same sample were recorded at different time. Cathode conditions: (a) under N_2 with RH = 90%, (b) under N_2 with RH = 100%, and (c) under 20% O_2/N_2 with RH = 90%.

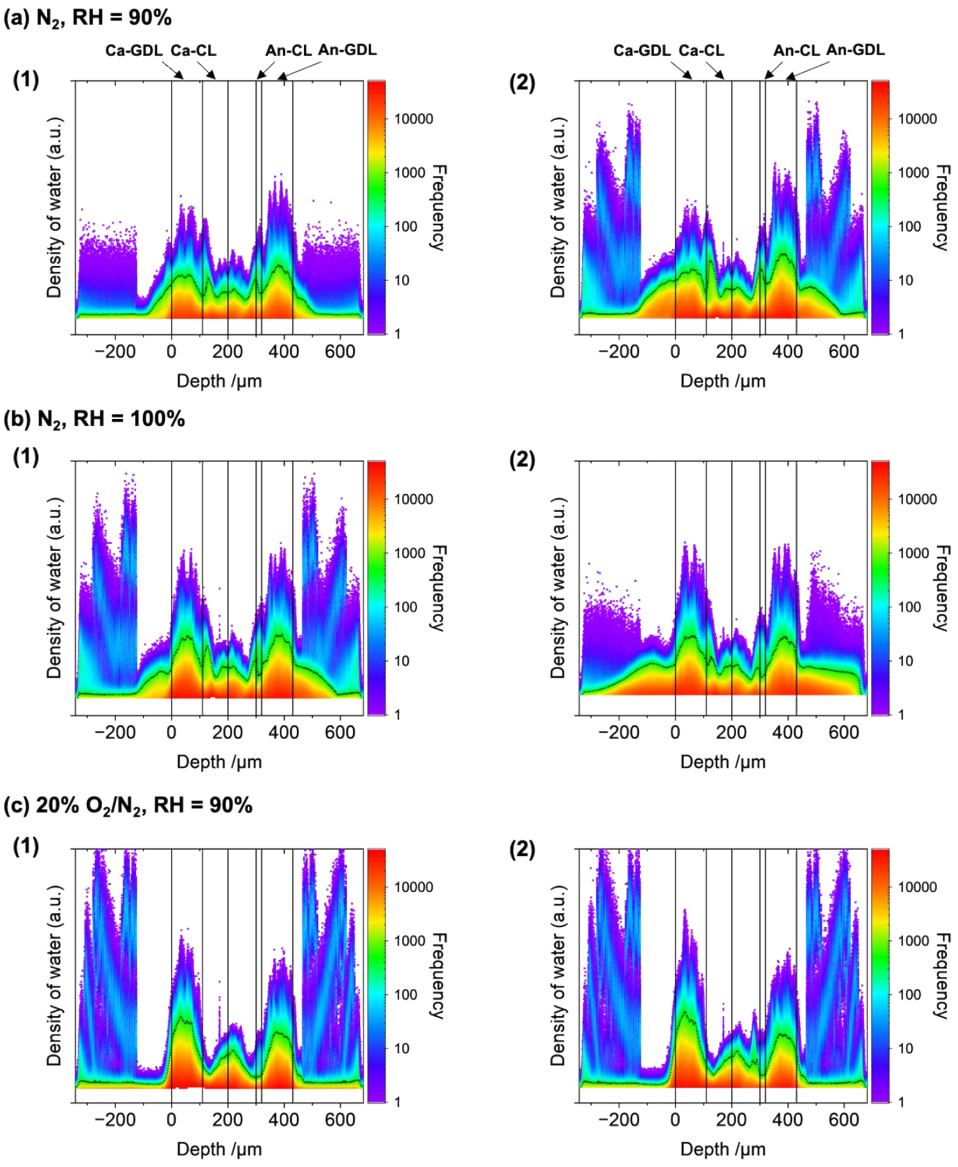

Fig. S6 Other examples of 2D histograms. Cathode conditions: (a) under N_2 with RH = 90%, (b) under N_2 with RH = 100%, and (c) under 20% O_2/N_2 with RH = 90%. The results correspond to the data in (1) and (2) of Fig. S5.

Supplementary Reference

[S1] H. M. Hudson, R. S. Larkin, *IEEE Trans. Med. Imaging*, **1994**, 13, 601.